JEM Journal of Experimental Medicine

ARTICLE

Uhrf1 regulates germinal center B cell expansion and affinity maturation to control viral infection

Chao Chen[1*], Sulan Zhai[1*], Le Zhang[1], Jingjing Chen[1], Xuehui Long[1], Jun Qin[2], Jianhua Li[3], Ran Huo[4], and Xiaoming Wang[1]

The production of high-affinity antibody is essential for pathogen clearance. Antibody affinity is increased through germinal center (GC) affinity maturation, which relies on BCR somatic hypermutation (SHM) followed by antigen-based selection. GC B cell proliferation is essentially involved in these processes; it provides enough templates for SHM and also serves as a critical mechanism of positive selection. In this study, we show that expression of epigenetic regulator ubiquitin-like with PHD and RING finger domains 1 (Uhrf1) was markedly up-regulated by c-Myc–AP4 in GC B cells, and it was required for GC response. Uhrf1 regulates cell proliferation–associated genes including *cdkn1a*, *slfn1*, and *slfn2* by DNA methylation, and its deficiency inhibited the GC B cell cycle at G1-S phase. Subsequently, GC B cell SHM and affinity maturation were impaired, and Uhrf1 GC B knockout mice were unable to control chronic virus infection. Collectively, our data suggest that Uhrf1 regulates GC B cell proliferation and affinity maturation, and its expression in GC B cells is required for virus clearance.

Introduction

During T cell–dependent humoral response induced by pathogen infection or immunization, antigen-activated B cells form a specialized transient structure in secondary lymphoid organs called the germinal center (GC; Allen et al., 2007). GC B cells cyclically migrate between dark zone (DZ) and light zone (LZ) and undergo clonal expansion and somatic hypermutation (SHM) in DZ followed by BCR affinity–based selection in LZ with only cells that have attained improved affinity for initiating antigen positively selected (Chan and Brink, 2012; De Silva and Klein, 2015; Mesin et al., 2016). This process is known as affinity maturation, whereby the affinity of serum antibodies increases over time so that the highly protective neutralizing antibodies are generated to control viral infections. Clonal expansion of GC B cells is critical for infection protection because it greatly expands the low-frequency antigen-specific B cells to ensure enough B cells and thus sufficient quantities of antibodies (Zhang et al., 2016b). More importantly, GC B cell proliferation also plays essential role in affinity maturation. On one hand, cell expansion provides large pool of templates for SHM and therefore is essential for accumulation of somatic mutations and diversification of BCR (Bergthorsdottir et al., 2001; Chan and Brink, 2012). On the other hand, cell proliferation is one of the major mechanisms for LZ GC B cells to be positively selected (Gitlin et al., 2015). After obtaining T cell help, selected LZ B cells undergo sustained and rapid proliferation in DZ with an accelerated cell cycle rate compared with unselected B cells, and thus are selectively expanded and further diversified (Gitlin et al., 2014, 2015). In terms of the latter process, recent studies identified c-Myc and its downstream AP4 as the essential regulators of the selection-driven proliferation, although how AP4 further promotes cell proliferation has not been completely addressed yet (Calado et al., 2012; Dominguez-Sola et al., 2012; Chou et al., 2016).

Uhrf1 (ubiquitin-like with PHD and RING finger domains 1, also known as Np95 or ICBP90) is an important epigenetic regulator containing multiple functional domains including Ubl, TTD, PHD, SRA (SET- and RING finger–associated domain), and RING and thus is involved in various cellular processes (Bostick et al., 2007; Nishiyama et al., 2013; Bashtrykov et al., 2014; Liang et al., 2015; Tian et al., 2015; Jia et al., 2016; Kent et al., 2016; Zhang et al., 2016a). One of the primary functions of Uhrf1 is to maintain DNA methylation and repress gene expression (Bostick et al., 2007; Sharif et al., 2007). Uhrf1 recognizes hemimethylated DNA generated during replication via its SRA domain and recruits DNA methyltransferase Dnmt1 to sustain the methylation of the newly synthesized DNA strand (Liu et al., 2013). Uhrf1 also possesses the ubiquitin ligase activity by virtue of its RING domain and

[1]Department of Immunology, State Key Laboratory of Reproductive Medicine, Nanjing Medical University, Nanjing, China; [2]Key Laboratory of Stem Cell Biology, Chinese Academy of Sciences Center for Excellence in Molecular Cell Science, Institute of Health Sciences, Shanghai Institutes for Biological Sciences, Chinese Academy of Sciences/Shanghai Jiao Tong University School of Medicine, Shanghai, China; [3]Key Laboratory of Medical Molecular Virology, Department of Medical Microbiology, Shanghai Medical College, Fudan University, Shanghai, China; [4]State Key Laboratory of Reproductive Medicine, Department of Histology and Embryology, Nanjing Medical University, Nanjing, China.

*C. Chen and S. Zhai contributed equally to this paper; Correspondence to Xiaoming Wang: xmwang@njmu.edu.cn.

© 2018 Chen et al. This article is distributed under the terms of an Attribution–Noncommercial–Share Alike–No Mirror Sites license for the first six months after the publication date (see http://www.rupress.org/terms/). After six months it is available under a Creative Commons License (Attribution–Noncommercial–Share Alike 4.0 International license, as described at https://creativecommons.org/licenses/by-nc-sa/4.0/).

Downloaded from http://rupress.org/jem/article-pdf/215/5/1437/1758913/jem_20171815.pdf by guest on 07 February 2026

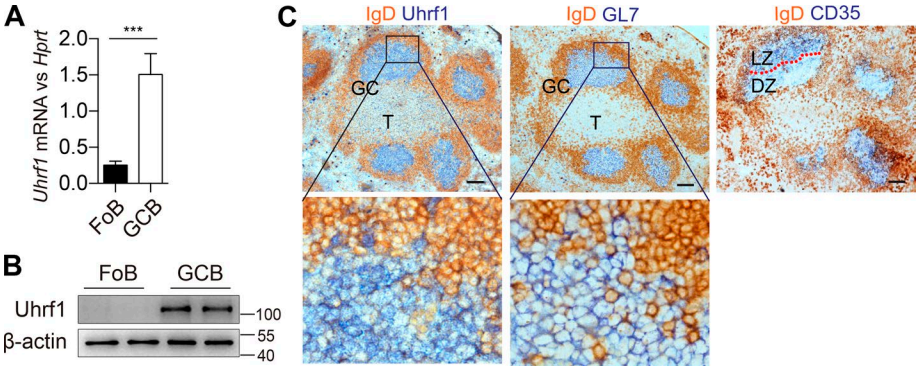

Figure 1. **Uhrf1 is specifically expressed in GC B cells. (A)** RT-qPCR analysis of Uhrf1 transcripts from FoBs and GC B cells. $n = 3$. Error bars show means ± SEM. ***, $P < 0.001$. **(B)** Western blot of Uhrf1 proteins in FoB and GC B cells. Molecular weight is indicated in kilodaltons. **(C)** Immunohistochemistry analysis of serial splenic sections for SRBC-immunized mice. Anti-IgD stains for FoBs, anti-CD35 stains for follicular dendritic cells (LZ), and GL7 stains for GC B cells. T, T cell zone. Bars, 100 µm. Data are representative of two experiments.

mediates ubiquitination of either histone or nonhistone proteins (Nishiyama et al., 2013; Zhang et al., 2016a). Previous research reveals critical roles of Uhrf1 in regulatory T cell proliferation, hematopoietic stem cell fate decision, and natural killer T cell survival and differentiation and so on (Obata et al., 2014; Cui et al., 2016; Zhao et al., 2017), indicating that Uhrf1 has potentially distinct biological functions dependent on cellular contexts. However, the role of Uhrf1 in B cell differentiation, especially in GC response, has not been investigated yet. To explore this, we generated GC B cell–specific KO mice and found that Uhrf1 is critically required for GC B cell proliferation and affinity maturation, and Uhrf1$^{GCB\ KO}$ mice are not able to efficiently control chronic virus infection.

Results

Uhrf1 is specifically expressed in GC B cells

We first examined the expression of Uhrf1 by real-time quantitative PCR (RT-qPCR) and found that Uhrf1 was up-regulated in GC B cells compared with naive follicular B cells (FoBs; Fig. 1 A). Western blot further confirmed the up-regulated protein of Uhrf1 in GC B cells (Fig. 1 B). The striking difference of Uhrf1 expression between GC B cells and FoBs was also evident by immunohistochemistry staining, making Uhrf1 a marker to identify GC regions on tissue sections of secondary lymphoid organs (Fig. 1 C). Uhrf1 was expressed in both LZ and DZ GC B cells (Fig. 1 C). The specificity of Uhrf1 antibody was validated by complete lack of staining in the GCs of *Uhrf1*$^{fl/fl}$ activation-induced cytidine deaminase (AID)-Cre^{+} mice (Fig. 3 B).

c-Myc–AP4 directly up-regulates Uhrf1 expression in GC B cells

The highly expressed Uhrf1 in GC B cells was remarkable (Fig. 1, A–C). We then therefore investigated how it was up-regulated in GC B cells. One of the primary biological functions of Uhrf1 is to promote cell proliferation (Obata et al., 2014; Xiang et al., 2017), which is a critical event for GC B cell response. c-Myc is transiently induced by follicular helper T cells in positively selected GC B cells to promote them to enter cell cycle (Calado et al., 2012; Dominguez-Sola et al., 2012). Sustained AP4 expression downstream of c-Myc further supports GC B cell proliferation and plays an essential role in GC B cell SHM and affinity maturation (Chou et al., 2016). Using membrane CD40L, we confirmed the sequential induction of c-Myc and AP4 expression (Fig. 2 A). Interestingly, we found that Uhrf1 expression was also induced by membrane CD40L after AP4 induction (Fig. 2 A), which led us to hypothesize that Uhrf1 might be downstream of the c-Myc–AP4 axis. In support of this hypothesis, published RNA sequencing (RNA-seq) data suggested that the Uhrf1 transcript was more abundant in AP4-positive GC B subsets than in AP4-negative subsets (Fig. 2 B; Chou et al., 2016). Moreover, both c-Myc and AP4 are required for Uhrf1 expression, and either c-Myc or AP4 shRNA knockdown led to significant reduction of Uhrf1 (Fig. 2, C and D).

To address whether AP4 directly regulates Uhrf1 expression, we reanalyzed the anti-AP4 chromatin immunoprecipitation assay (ChIP) sequencing (ChIP-seq) data (Chou et al., 2016) and were able to identify two binding peaks of AP4 near the transcriptional start site of the *Uhrf1* gene locus (Fig. 2 E). Examination of DNA sequence of *Uhrf1* gene revealed that these two AP4 binding peaks corresponded with two conserved AP4 binding motifs (CAGCTG; Fig. 2, E and F). By ChIP-qPCR, we confirmed that AP4 indeed occupied these two sites in the Uhrf1 gene locus in both CH12F3 cells and GC B cells (Fig. 2 G). In addition, a luciferase reporter assay was performed to corroborate these findings (Fig. 2 H). AP4 expression markedly enhanced Uhrf1 luciferase reporter activity, and this up-regulation was fully dependent on the two conserved AP4 binding motifs because their mutations completely abrogated AP4 mediated up-regulation of Uhrf1 promoter activity (Fig. 2 H). We then performed a rescue experiment by overexpressing Uhrf1 in AP4 shRNA knocked-down GC B cells. To enable in vitro–activated B cells to participate in GC response, we adoptively transferred retrovirally transduced polyclonal B cells into MD4 BCR transgenic mice and then immunized the mice with sheep RBCs (SRBCs; Muppidi et al., 2014). As shown in Fig. 2 I, AP4 shRNA indeed reduced the GC response, and importantly, this reduction could be rescued by Uhrf1 overexpression. Collectively, our data suggest that the c-Myc–AP4 axis directly up-regulated Uhrf1 expression in GC B cells.

Uhrf1 is required for GC B cell response

To investigate the role of Uhrf1 in GC response, *Uhrf1*$^{fl/fl}$ mice were crossed with transgenic AID-Cre mice. In obtained *Uhrf1*$^{fl/fl}$ AID-Cre^{+} mice, only active B cells were depleted of Uhrf1 and thereafter referred to as Uhrf1$^{GCB\ KO}$ mice (Kwon et al., 2008). As a transgene, AID-Cre has no effect on GC response (Pérez-García et al., 2017), therefore we used *Uhrf1*$^{fl/fl}$ mice as the control, and they were referred to as WT or Uhrf1$^{GCB\ WT}$ mice. When WT

Downloaded from http://rupress.org/jem/article-pdf/215/5/1437/1758913/jem_20171815.pdf by guest on 07 February 2026

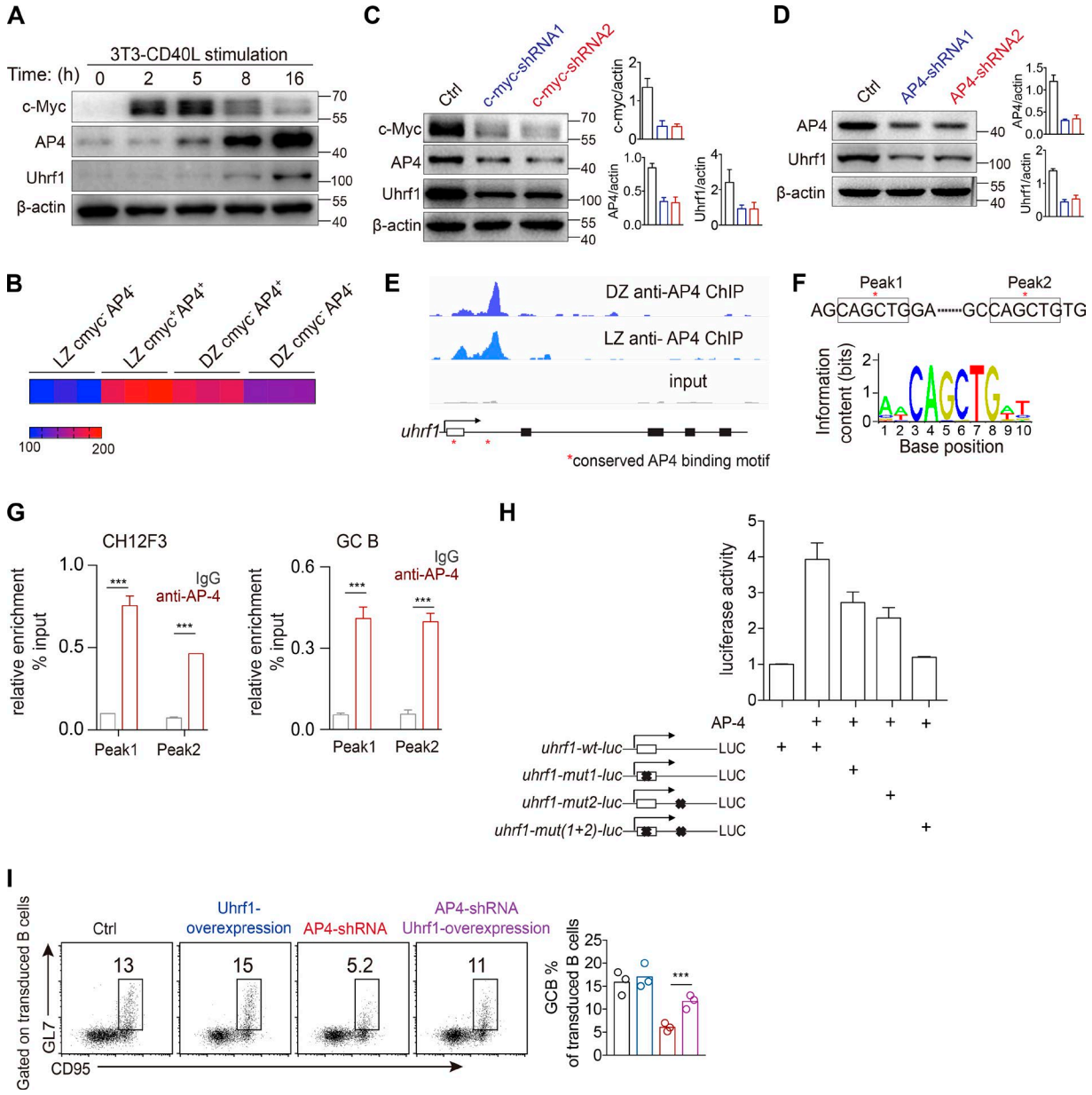

Figure 2. **c-Myc–AP4 directly up-regulates Uhrf1 expression in GC B cells. (A)** Primary B cells were stimulated on the CD40L-expressing feeders. Dynamic induction of c-Myc, AP4, and Uhrf1 were assessed with Western blotting. **(B)** Uhrf1 expression in subsets of GC B cells. Data were from GSE80669 (Chou et al., 2016). **(C)** Western blot analysis of AP4 and Uhrf1 expression in c-Myc shRNA transfected CH12F3 B cell lines. **(D)** Western blot analysis of Uhrf1 expression in AP4 shRNA-transfected CH12F3 B cell lines. Molecular weight is indicated in kilodaltons. **(E)** Snapshot of AP4 ChIP-Seq signals at Uhrf1 gene locus in GC B cells (from GSE80669; Chou et al., 2016). **(F)** Conserved AP4 binding sequence. Red asterisks indicate conserved AP4 binding sites. **(G)** ChIP-qPCR validation of AP4 binding at Uhrf1 gene locus with CH12F3 cells (left) and GC B cells (right). **(H)** AP4 promotes Uhrf1 transcription in luciferase (LUC) reporter assay. WT or AP4 binding site mutant Uhrf1 promoter luciferase reporter vectors were cotransfected with AP4 expression plasmid into 293T cells, and luciferase activity was measured as a function of AP4-dependent Uhrf1 transcription. **(I)** In vitro–activated B cells were transduced with retroviral shRNA or Uhrf1 as indicated, adoptively transferred into MD4 BCR transgenic mice, and then immunized with SRBCs for 7 d. GC response of transduced B cells was analyzed by flow cytometry. Data are representative of three (A, C, D, and H) or two (G and I) experiments. Error bars show means ± SEM. ***, P < 0.001.

and Uhrf1$^{GCB\ KO}$ mice were immunized with model SRBCs, we found approximately fivefold reduction of splenic GC response in Uhrf1$^{GCB\ KO}$ mice compared with the WT control (Fig. 3 A). Similar reduction was seen in chronic GC B cell response in response to commensal flora in mesenteric LNs and Peyer's patch (Fig. 3 A). The disrupted GC response in Uhrf1$^{GCB\ KO}$ mice was also evident by immunohistochemistry analysis (Fig. 3 B). Uhrf1 staining revealed complete depletion efficiency in KO cells (Fig. 3 B). Further analysis showed a slight impairment of IgG1 class switch in Uhrf1$^{GCB\ KO}$ mice (Fig. 3 C). Despite the striking reduced GC response, GC B cells in Uhrf1$^{GCB\ KO}$ mice were still bona fide GC B cells because they retained normal level of Bcl6, the master regulator of GC B cells (Fig. 3 D; Basso and Dalla-Favera, 2010). To mimic more physiological immune responses, mice were infected with lymphocytic choriomeningitis virus (LCMV)–Armstrong virus instead of model

Downloaded from http://rupress.org/jem/article-pdf/215/5/1437/1758913/jem_20171815.pdf by guest on 07 February 2026

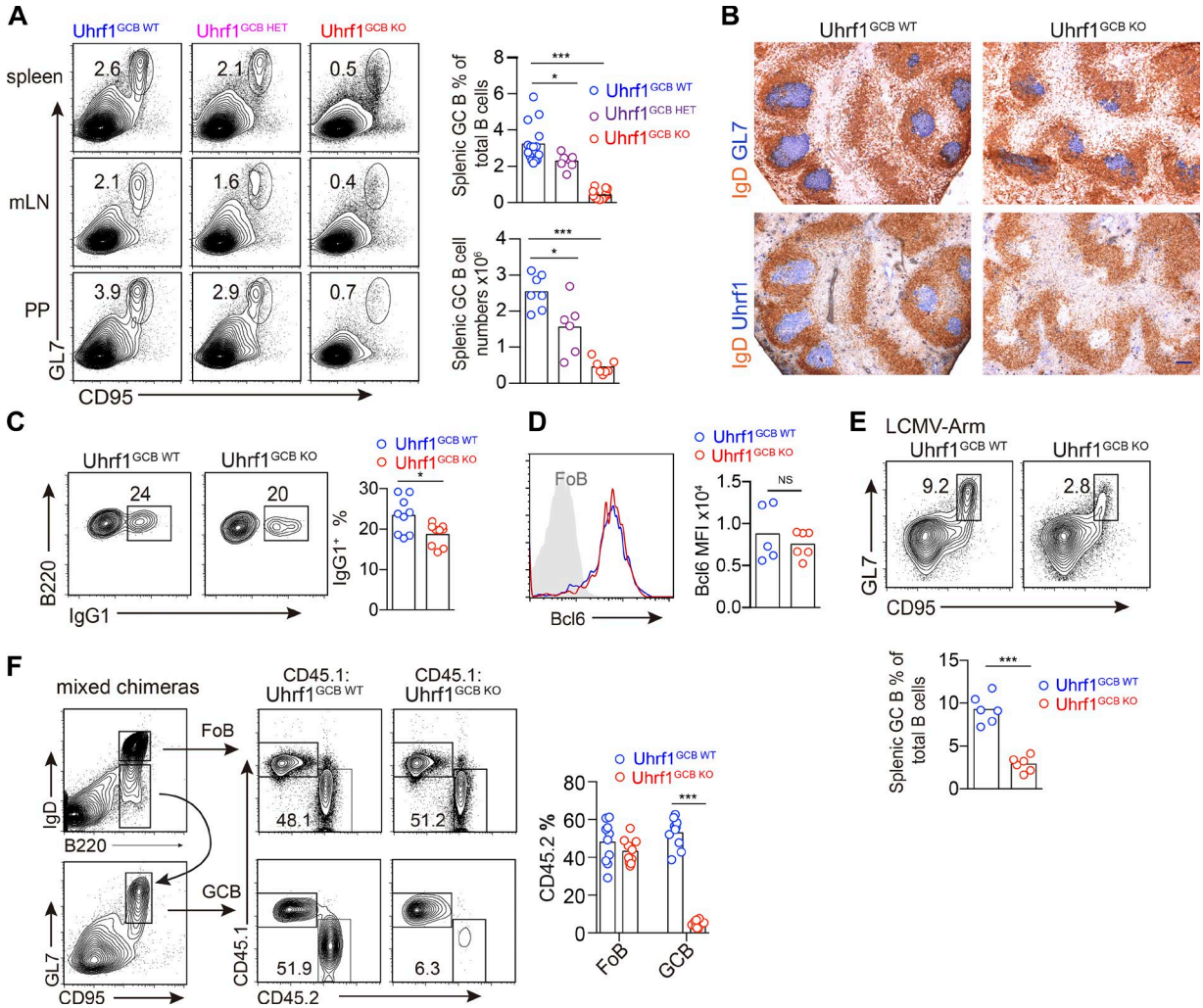

Figure 3. **Uhrf1 is required for GC response. (A, B, and D)** Mice of each genotype were immunized with SRBCs and analyzed at day 8. **(A)** Flow cytometric analysis of GC B cells (B220⁺CD95⁺GL7⁺) in spleen, mesenteric LN (mLN), and Peyer's patches (PPs) from Uhrf1 WT, heterozygous, and KO mice. Data were pooled from three experiments. *n* = 6–10. **(B)** Cryosections from each genotype of mice were immunohistochemically stained for GC B cells (anti-GL7) and Uhrf1 expression (anti-Uhrf1, bottom in blue). Data are representative of three experiments. Bar, 100 µm. **(C)** Flow cytometry analysis of IgG1 class switch in GC B cells. *n* = 9. Data were pooled from four experiments 7 or 10 d after SRBC immunization. **(D)** Bcl6 expression were intracellularly stained by flow cytometry in GC B cells. Data were pooled from two experiments. *n* = 5–6. **(E)** Mice were infected with LCMV-Armstrong (LCMV-Arm) and analyzed for splenic GC B cells at day 12. Data were pooled from two experiments. *n* = 6. **(F)** Mixed BM chimeras generated with ~50% Uhrf1^{GCBWT} or Uhrf1^{GCBKO} CD45.2 cells,~50% CD45.1 WT cells were immunized with SRBCs, and the percentage of CD45.2⁺ FoB and GC B cells was analyzed by flow cytometry. Data were pooled from two experiments. In all bar graphs, bars represent means, and dots represent individual mice. Error bars show means ± SEM. *, P < 0.05; ***, P < 0.001.

antigens. We still found a strong reduction of GC B cell response in this circumstance (Fig. 3 E). Finally, to ask whether the GC response defect in the absence of Uhrf1 is intrinsic to the B cell compartment, we generated 50:50 mixed bone marrow (BM) chimera using CD45.1 WT and CD45.2 Uhrf1$^{GCB\ WT}$ or Uhrf1$^{GCB\ KO}$ donors and analyzed the contributions of CD45.2⁺ Uhrf1$^{GCB\ WT}$ or Uhrf1$^{GCB\ KO}$ cells to follicular B and GC B compartments. As shown in Fig. 3 F, Uhrf1$^{GCB\ KO}$ cells normally contributed to the FoB compartment, whereas their contribution to the GC B cell compartment was greatly reduced. The reduction was even stronger than in the nonchimeric mice, potentially because of the property of competitive setting in mixed chimeras. Collectively, our data showed that Uhrf1 is required for GC B cell response in a cell-intrinsic manner, in response to both model antigen and virus infection.

Uhrf1 loss impaired GC B cell proliferation without affecting cell survival

We then aimed to understand how Uhrf1 loss impaired GC B cell response. Given that Uhrf1 is up-regulated by the c-Myc–AP4 axis, the essential regulator of GC B cell proliferation, we therefore first analyzed whether Uhrf1 deficiency affected GC B cell proliferation. Flow cytometry analysis of DNA content showed that Uhrf1-defecient GC B cells harbored a larger proportion of cells in G1 phase and a smaller proportion in S phase (Fig. 4 A), suggesting a cell cycle delay at the G1-S transit. Consistently, BrdU incorporation analysis revealed a reduced cell proliferation rate in Uhrf1 KO GC B cells (Fig. 4 B). We next adopted a 5-ethynyl-2′-deoxyuridine (Edu)-BrdU sequential labeling methodology to examine the cell cycle defect at a higher resolution and discriminate early S– (Edu⁻BrdU⁺), mid/late S– (Edu⁺BrdU⁺) and

Downloaded from http://rupress.org/jem/article-pdf/215/5/1437/1758913/jem_20171815.pdf by guest on 07 February 2026

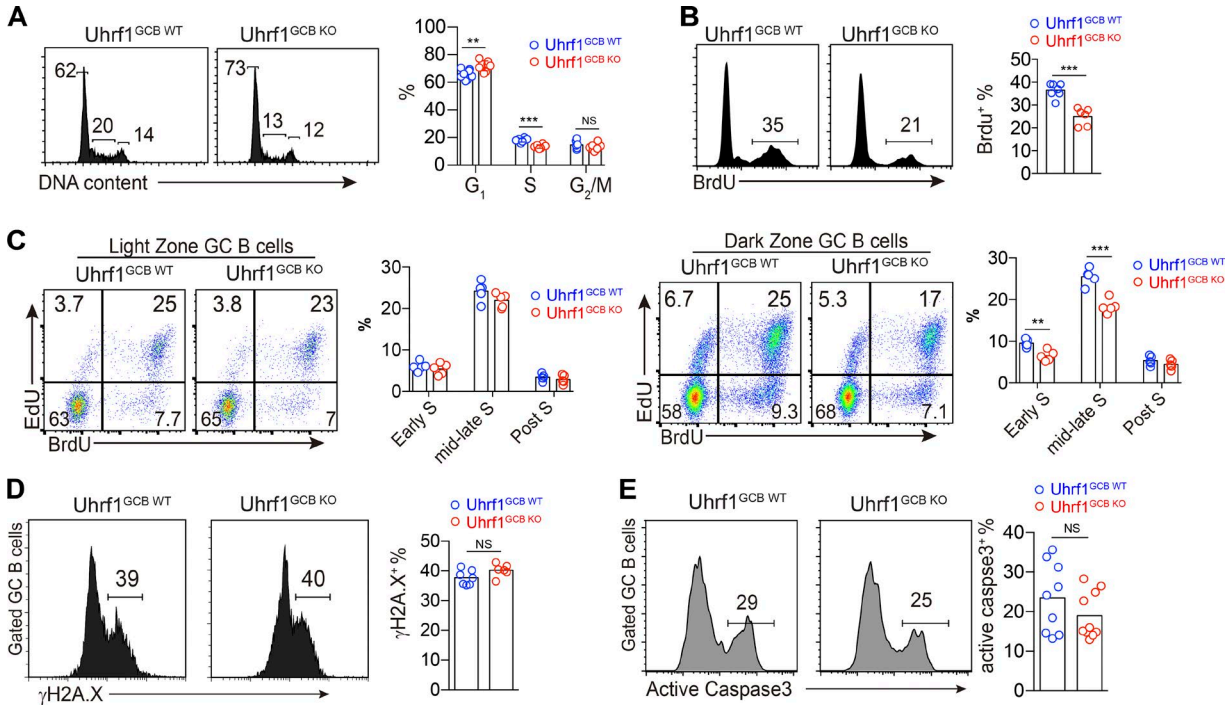

Figure 4. **Uhrf1 loss impaired GC B cell proliferation without affecting cell survival. (A–E)** Mice of each genotype were immunized with SRBCs and analyzed at days 7–10. **(A)** Cell cycle of GC B cells were analyzed by DNA content staining. *n* = 6. **(B)** Flow cytometry analysis of GC B cell BrdU incorporation 30 min after BrdU treatment. *n* = 6. **(C)** Mice were pulsed with Edu followed 1 h later by BrdU, and mice were then analyzed at 0.5 h after BrdU pulse for BrdU-Edu double staining. *n* = 5–6. **(D)** Representative dot plots of γH2a.X staining profile in GC B cells. *n* = 6. **(E)** Frequency of GC B cells with activated caspase 3 were analyzed by flow cytometry. Data were pooled from three (A, C, and E) or two (B and D) experiments. *n* = 9. In all bar graphs, bars represent means, and dots represent individual mice. **, P < 0.01; ***, P < 0.001.

post-S– (Edu⁺BrdU⁻) phase cells (Gitlin et al., 2015; Chen et al., 2017). As shown in Fig. 4 C, the proportions of early S and mid/late S cells were significantly reduced in Uhrf1-deficent DZ GC B cells, but not in LZ GC B cells, reminiscent of the cell cycle defect phenotype in AP4 KO GC B cells (Chou et al., 2016).

A previous study reported that compared with WT control, Dnmt1-deficient GC B cells accumulated more DNA damage as indicated by increased γH2A.X staining and therefore were more prone to apoptosis (Shaknovich et al., 2011). We examined DNA damage in Uhrf1-deficient mice and observed a comparable level of γH2A.X positive GC B cells between WT and KO mice (Fig. 4 D). Consistently, there was no detectable difference in GC B cell apoptosis between WT and Uhrf1-deficient mice (Fig. 4 E). These data suggest that Uhrf1 enhanced GC B cell proliferation by promoting cell cycle G1-S transition, whereas it was dispensable for GC B cell survival, indicating deferential roles of Uhrf1 and Dnmt1 in GC B cells.

Uhrf1 promotes GC B cell proliferation via *Cdkn1a* DNA methylation

One of the major functions of Uhrf1 is to maintain DNA methylation by recruiting Dmnt1. Indeed, Uhrf1-deficient GC B cells harbored less methylated DNA than the WT control (Fig. 5 A). To gain insight into the molecular mechanism by which Uhrf1 regulated GC B cell proliferation, we conducted gene expression profile analysis by RNA-seq of WT and Uhrf1-deficient GC B cells. Gene Ontology (GO) enrichment analysis identified multiple cell proliferation–associated pathways (Fig. S1 A). When comparing AP4 targets with Uhrf1 targets, ~10% of AP4 targets seemed to be Uhrf1-dependent (Fig. S1 B). Among all the Uhrf1 targets, there were more up-regulated than down-regulated genes (Fig. 5 B), suggesting that Uhrf1 might primarily inhibit gene expression via DNA methylation in GC B cells.

A previous study showed that Uhrf1 was responsible for DNA methylation of *Cdkn1a* (encoding p21 protein) and inhibits its expression in regulatory T cells (Obata et al., 2014), leading us to speculate whether Uhrf1 mediates methylation of Cdk inhibitor family proteins in GC B cells. Focusing on the Cdk inhibitor family, we found that Cdkn1a expression was markedly up-regulated in the Uhrf1-deficient GC B cells (Fig. 5 C). Real-time-qPCR further confirmed this up-regulation (Fig. 5 D). Bisulfite sequencing analysis was then performed to assess the DNA methylation status of *Cdkn1a*, and we found that CpG sites of *Cdkn1a* gene showed a decreased DNA methylation level in Uhrf1-deficient GC B cells than in WT GC B cells (Fig. 5 E). This decreased DNA methylation potentially led to increased p21 expression. To validate whether p21 inhibition was the molecular mechanism by which Uhrf1 promoted a GC response, we conducted rescue experiments by knocking down p21 in Uhrf1-deficient cells. BM hematopoietic stem cells from Uhrf1$^{GCB\,KO}$ mice were retrovirally transduced with p21 shRNA or control vector, and these hematopoietic stem cells were then used as donor cells to generate BM chimeras (Fig. 5 F). Upon SRBCs immunization, Uhrf1-deficient cells formed significantly stronger (approximately threefold) GC response in chimeras transduced with p21 shRNA vector than in control vector chimeras (Figs. 5 G and S2), meaning that p21 knockdown could rescue

Downloaded from http://rupress.org/jem/article-pdf/215/5/1437/1758913/jem_20171815.pdf by guest on 07 February 2026

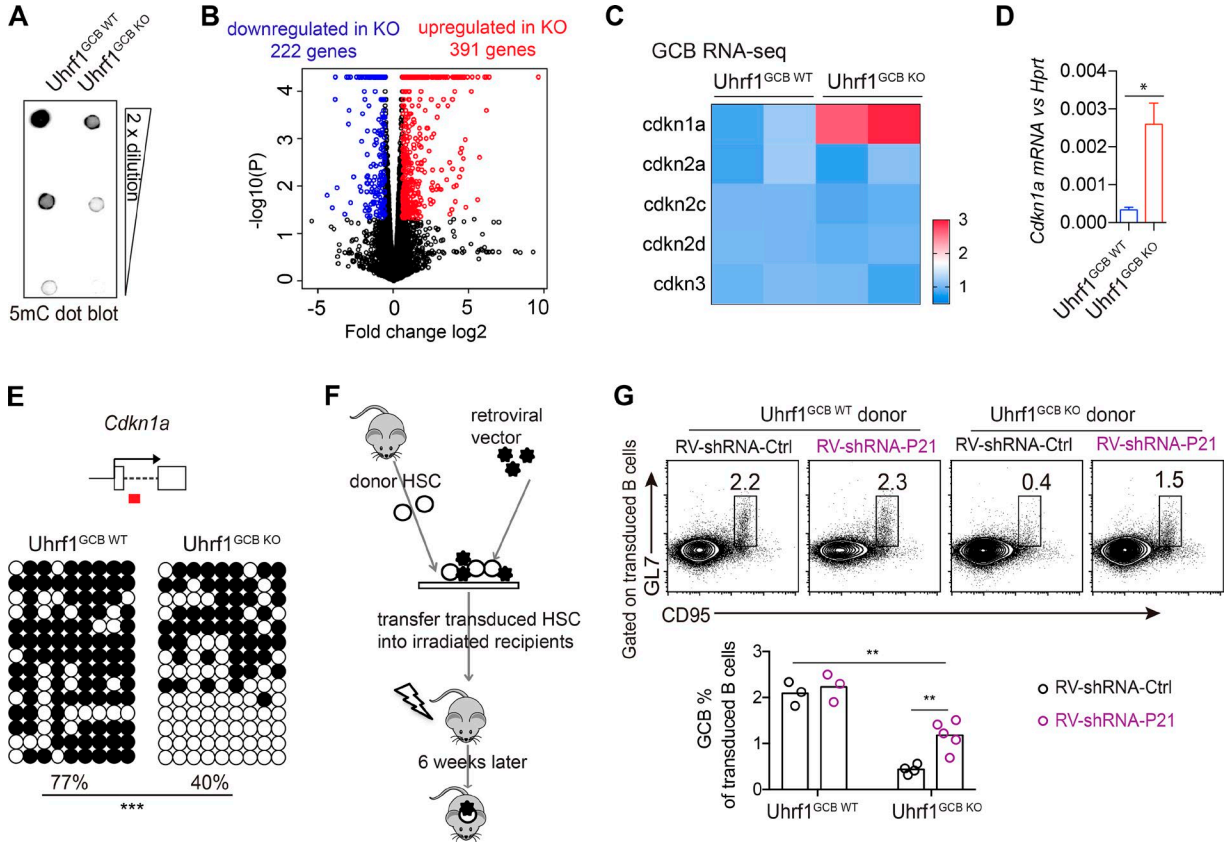

Figure 5. **Uhrf1 promotes GC B cell proliferation via *Cdkn1a* DNA methylation. (A)** Dot blot analysis of total 5mC in genomic DNA extracted from GC B cells of each genotype. **(B)** Comparison of all differentially expressed genes ($P < 0.05$; fold change > 1.5) in GC B cells from Uhrf1 WT and KO mice from RNA-seq analysis. **(C)** Heat map depicting the relative expression change of Cdk inhibitors in the absence of Uhrf1 in GC B cells. Data were from RNA-seq analysis. **(D)** RT-qPCR analysis of *Cdkn1a* transcripts in GC B cells. $n = 3$. **(E)** Methylation analysis of *Cdkn1a* was performed by bisulfite conversion of genomic DNA extracted from FACS-sorted WT and Uhrf1-deficient GC B cells. The selected genomic region is shown by red bar. Open circles, unmethylated; filled circles, methylated. The frequencies of methylation are shown below. Each row represents one bacterial clone, and each column represents one CpG site. Statistical analysis was done with Fisher's exact test. **(F and G)** BM cells of WT or Uhrf1^{GCBKO} mice were transduced with retrovirus expressing control shRNA or *Cdkn1a* shRNA and used as donors to generate BM chimeric mice (F). The frequency of GC B cells (CD95$^+$GL7$^+$) in transduced B cells of SRBCs-immunized chimeric mice was analyzed by flow cytometry (G). Statistical analysis was done with one-way ANOVA. Data are representative of two experiments. HSC, hematopoietic stem cell. In all bar graphs, bars represent means, and dots represent individual mice. Error bars show means ± SEM. *, $P < 0.05$; **, $P < 0.01$; ***, $P < 0.001$.

the Uhrf1 deficiency–mediated GC reduction. However, this rescue seems to be partial, and the GC frequency of p21 knocked-down Uhrf1-deficient cells was still lower than that of Uhrf1-sufficient cells (Fig. 5 G). Collectively, Uhrf1 promotes GC B cell proliferation at least partially through maintaining *Cdkn1a* DNA methylation.

Uhrf1 methylates the *Schlafen 1/2* (*Slfn1/2*) gene locus to promote GC B cell proliferation

Given that *Cdkn1a* DNA methylation might only partially account for the GC response defect in the absence of Uhrf1, we then aimed to identify other targets by which Uhrf1 regulates GC B cell proliferation. The *Slfn* family is a set of evolutionally conserved genes, with the name meaning "to sleep" in German (Liu et al., 2017). There are at least 10 members in the mouse, and among these genes, *Slfn1*, *2*, and *8* have been reported to be associated with cell proliferation or cell senescence maintenance (Schwarz et al., 1998; Geserick et al., 2004; Berger et al., 2010). By RNA-seq and RT-qPCR, we found that Slfn1, 2, and 8 were all up-regulated in Uhrf1$^{GCB\ KO}$ mice (Fig. 6 A). Bisulfite sequencing analysis revealed that the DNA methylation levels of *Slfn1* and *Slfn2* gene loci were significantly lower in Uhrf1$^{GCB\ KO}$ mice than in control mice (Fig. 6, B and C), suggesting that Slfn1 and Slfn2 are the direct targets of Uhrf1 in GC B cells. The DNA methylation level of *Slfn8* gene was rather low in GC B cells and not altered by Uhrf1 loss (Fig. 6 D), indicating that it's not regulated by means of DNA methylation. BM transduction experiments with shRNA targeting Slfns revealed that knocking down Slfn1 or Slfn2 could rescue the GC response (Figs. 6 E and S2). As a control, knocking down Slfns in WT cells had no impact on GC response.

One caveat of the above rescue experiments with BM chimeras is that knocking down p21 and Slfns early in BM progenitors could affect the B or T cell development, which might then influence GC response in a manner independent of Uhrf1 deficiency. To address this issue, we also performed rescue experiments by shRNA knocking down in mature B cells as done in Fig. 2 I. Consistent with the BM chimeras experiment, we found that either p21, Slfn1, or Slfn2 shRNA knockdown could significantly increase the GC of Uhrf1-deficient cells (Fig. S3).

By suppressing cell cycle entry, Slfns are critical for maintaining cell quiescence, and their expression level is thus dynamically

Downloaded from http://rupress.org/jem/article-pdf/215/5/1437/1758913/jem_20171815.pdf by guest on 07 February 2026

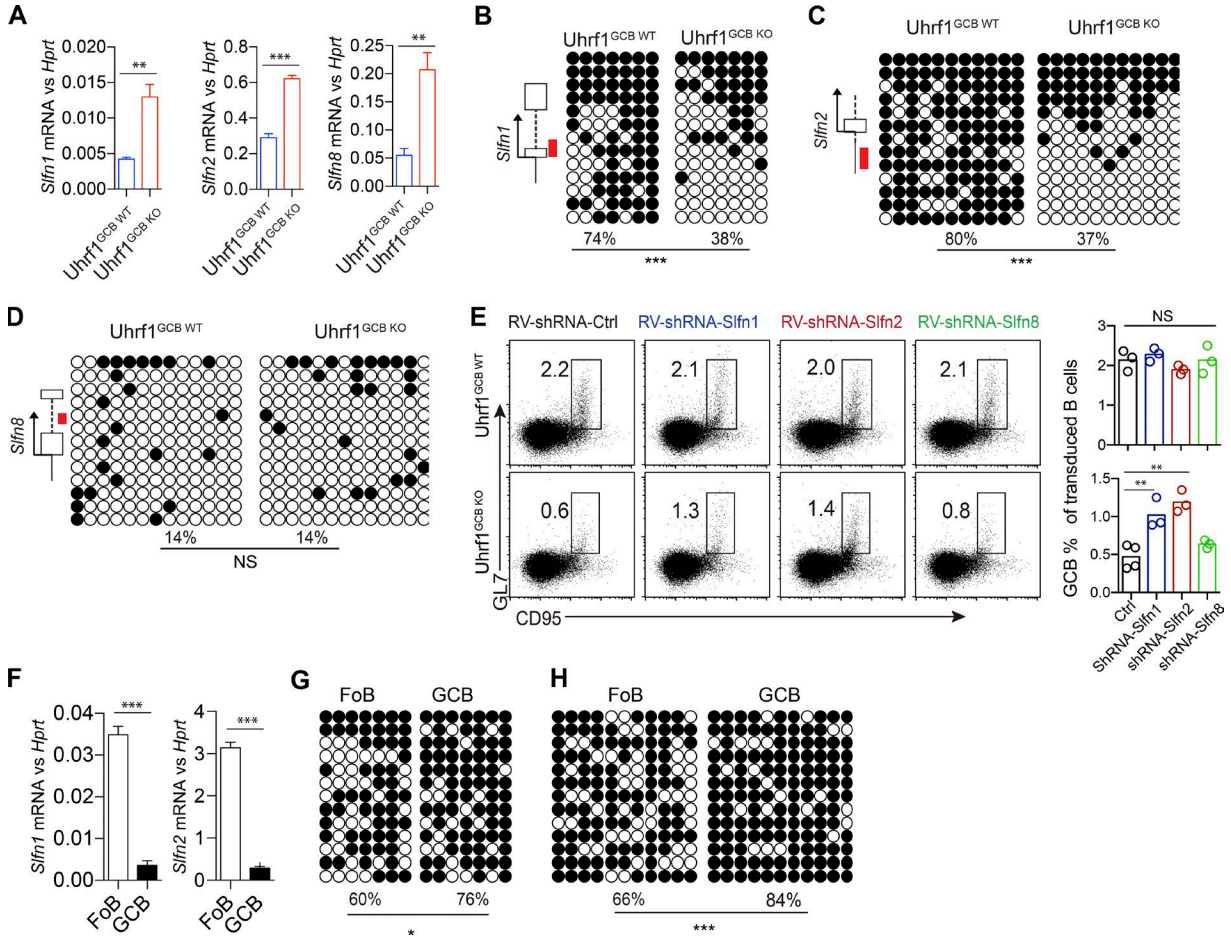

Figure 6. **Uhrf1 methylates Slfn1/2 gene locus to promote GC B cell proliferation. (A)** RT-qPCR analysis of *Slfn* transcripts in GC B cells. $n = 3$. **(B–D)** Methylation analysis of *Slfn1* (B), *Slfn2* (C), *and Slfn8* (D) were performed by bisulfite conversion of genomic DNA extracted from FACS-sorted WT and Uhrf1-deficient GC B cells. The selected genomic region is shown by a red bar. Open circles, unmethylated; filled circles, methylated. The frequencies of methylation are shown below. Statistical analysis was done with Fisher's exact test. **(E)** BM cells of Uhrf1^{GCBWT} and Uhrf1^{GCBKO} mice were transduced with retrovirus expressing control shRNA or Slfn shRNA and used as donors to generate BM chimeric mice as done in Fig. 5 F. Chimeric mice were immunized with SRBC 6 wk after reconstitution, and the frequency of GC B cells (CD95$^+$GL7$^+$) in transduced B cells of chimeric mice was analyzed by flow cytometry at day 7. $n = 3$. Statistical analysis was done with one-way ANOVA. **(F)** RT-qPCR analysis of *Slfn1* and *Slfn2* transcripts in sorted follicular and GC B cells. $n = 3$. **(G and H)** Methylation analysis of *Slfn1* (G) and *Slfn2* (H) was performed by bisulfite conversion of genomic DNA extracted from FACS sorted FoB and GC B cells as in B–D. Statistical analysis was done with Fisher's exact test. Data are representative of two (B–F) or three (A, G, and H) experiments. Error bars show means ± SEM. *, $P < 0.05$; **, $P < 0.01$; ***, $P < 0.001$.

regulated accordingly with the status of cell activation during T cell differentiation (Schwarz et al., 1998). We therefore assessed the expression of Slfn genes in naive FoBs and GC B cells. RT-qPCR analysis revealed that the transcripts of *Slfn1* and *Slfn2* was significantly reduced when B cells differentiated from naive cells into GC B cells (Fig. 6 F), and bisulfite sequencing analysis showed more DNA methylation of *Slfn1* and *Slfn2* gene in GC B cells (Fig. 6, G and H), consistent with higher expression of Uhrf1 in GC B cells. These data suggest that Uhrf1 was actively up-regulated in GC B cells to inhibit Slfn1 and Slfn2 expression and promote cell entry into the cell cycle.

Uhrf1 loss compromised GC B cell SHM and affinity maturation

By regulating GC B cell proliferation and expansion, the c-Myc–AP4 axis promotes SHM and ensures affinity maturation (Chou et al., 2016). As a downstream target of c-Myc–AP4 and a regulator of GC B cell proliferation, we reasoned that Uhrf1 might be similarly required for optimal SHM and affinity maturation. We examined the BCR mutation frequency in NP-KLH–immunized Uhrf1 WT and KO mice by genomic DNA sequencing. WT and Uhrf1 KO GC B cells were sorted out for sequencing of IgH VH186.2, which encodes NP-specific antibody, and JH4 intronic region, which is not associated with affinity selection and is thus a pure indicator of SHM efficiency. The overall mutation frequency of both JH4 and VH186.2 was substantially decreased in the absence of Uhrf1 (Fig. 7 A), meaning that the SHM was severely impaired. *Aicda* mRNA and AID protein were comparable between WT and KO mice (Fig. 7, B and C), suggesting that the reduced mutation frequency in Uhrf1-deficient GC B cells was not a result of AID alteration. Notably, we found a greatly reduced fraction of Uhrf1-deficent GC B cell clones carrying the W33L or Y99G mutation, which encodes higher-affinity BCR for NP antigen (Fig. 7 D), indicating that Uhrf1 loss impaired the affinity maturation. To validate this notion, ELISA experiments were performed to measure serum NP binding antibody titers. The total NP specific antibodies (NP41 binding) were significantly

Downloaded from http://rupress.org/jem/article-pdf/215/5/1437/1758913/jem_20171815.pdf by guest on 07 February 2026

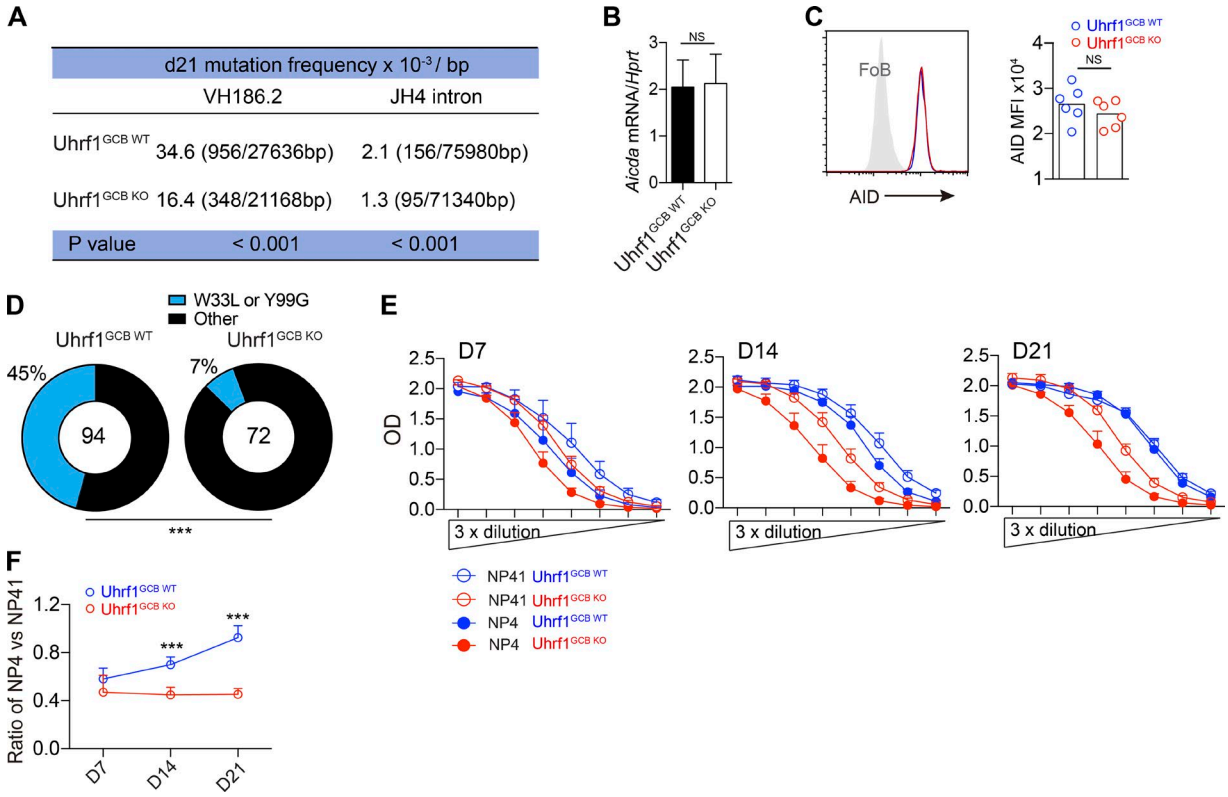

Figure 7. **Uhrf1 loss compromised GC B cell SHM and affinity maturation. (A–F)** Uhrf1$^{GCB\ WT}$ or Uhrf1$^{GCB\ KO}$ mice were immunized with NP-KLH and analyzed at time indicated. **(A)** Sorted GC B cells pooled from four mice of each genotype were used for the genomic DNA extraction and sequencing of VH186.2 exon and JH4 intronic region. Total mutation frequencies are shown. Statistical analysis was done with Fisher's exact test. **(B and C)** RT-qPCR (B) and intracellular flow cytometry analysis (C) of AID expression in GC B cells. **(D)** The frequency of W33L mutations in the VH186.2 heavy chain, was determined by sequencing. The total numbers of clones sequenced are indicated at the center of the pies. Statistical analysis was done with Fisher's exact test. **(E and F)** NP4 and NP41 binding antibodies in serum of immunized mice were analyzed by ELISA. OD value versus dilution factors are plotted (E). Ratios of NP4/NP41 were calculated with raw OD value in linear range (F). Statistical analysis was done with two-way ANOVA. Data are representative of three experiments. Error bars show means ± SEM. ***, P < 0.001.

reduced in Uhrf1$^{GCB\ KO}$ mice (Fig. 7 E), potentially because of decreased overall GC response. Interestingly, the higher-affinity antibodies (NP4-binding) were reduced to even a greater extent, and the ratio of NP4 versus NP41 antibody was markedly reduced in Uhrf1$^{GCB\ KO}$ mice (Fig. 7, E and F). This observation, in line with the reduced W33L mutation, indicated that Uhrf1-mediated cell proliferation was also critical for affinity-based selection. Collectively, Uhrf1 expression in GC B cells is essential for SHM and affinity maturation.

Uhrf1 is required for chronic virus clearance

Antibody response protects us against pathogen infections, and previous studies have demonstrated that the production of high-affinity antibody is indispensable for control of chronic LCMV infections (Bergthaler et al., 2009; Harker et al., 2011; Chou et al., 2016). Given the severely impaired GC response and antibody affinity maturation in the absence of Uhrf1, we infected the Uhrf1 WT and KO mice with chronic LCMV-cl13 to assess whether Uhrf1 loss in GC B cells leads to defective virus clearance. Not surprisingly, Uhrf1 deficiency significantly compromised GC B cell response (Fig. 8 A). LCMV-cl13 infection resulted in body weight loss in both Uhrf1 WT and KO mice. However, compared with WT mice, body weight of Uhrf1 GCB KO mice recovered significantly slower (Fig. 8 B), suggesting a defect in virus control. Indeed, by measuring the LCMV transcript, we found that the virus load in Uhrf1 GCB KO mice was much higher than in WT mice (Fig. 8 C). Collectively, our data demonstrate that Uhrf1 expression is indispensable for mounting an optimal GC response to control chronic LCMV virus.

Discussion

One of the primary functions of Uhrf1 is to recruit Dmnt1 for DNA methylation maintenance. A previous study has reported that Dnmt1 is required for the formation of GC response, and Dnmt1 loss led to increased double-strand DNA break and reduced GC B cells (Shaknovich et al., 2011). However, this study used Dnmt1 hypomorphic mice, which is a full deficiency setting, thus hampering detailed mechanistic study of the roles of Dnmt1 and DNA methylation in GC B cells. Uhrf1 is essential for the specificity of Dnmt1, but it's not very clear whether all of the Dnmt1-mediated DNA methylation events are dependent on Uhrf1 targeting (Bashtrykov et al., 2014). More complicated, both Uhrf1 and Dnmt1 have been reported to carry out functions in addition to DNA methylation (Robertson et al., 2000; Espada et al., 2011; Liang et al., 2015; Tian et al., 2015; Kent et al., 2016). Uhrf1 could even

Downloaded from http://rupress.org/jem/article-pdf/215/5/1437/1758913/jem_20171815.pdf by guest on 07 February 2026

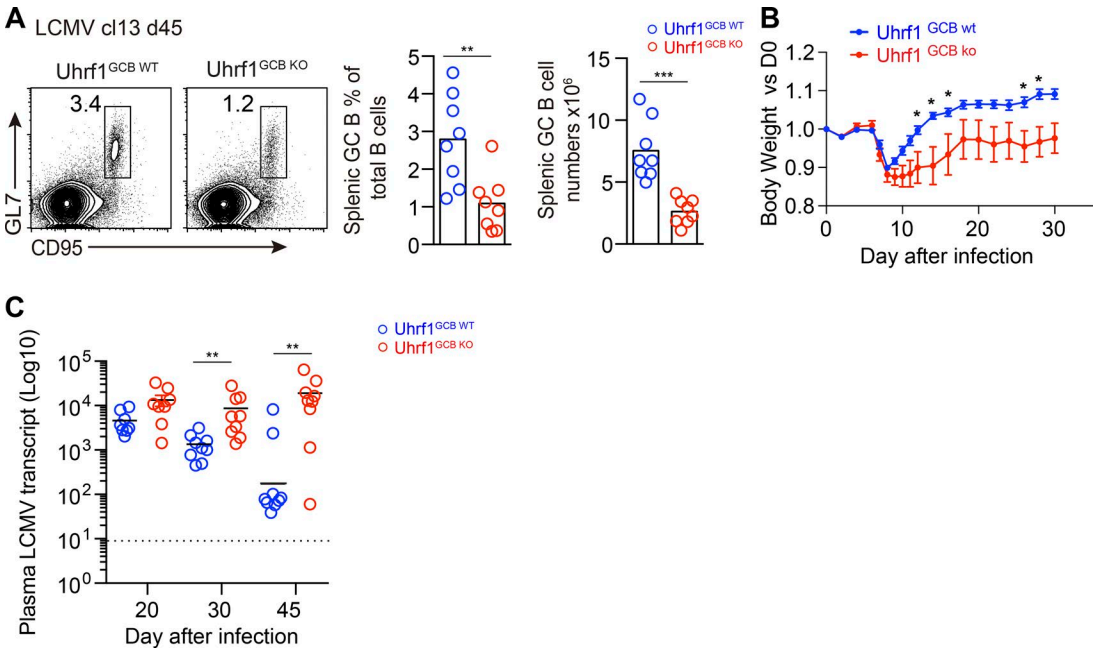

Figure 8. **Uhrf1 in GC B cells is required for control of chronic LCMV infection. (A)** GC B cell frequency and number in mice infected with LCMV cl13 were assessed by flow cytometry at day 40. *n* = 8. **(B)** Body weight before and after infection. Results are presented relative as original body weight (day 0; D0). *n* = 9. **(C)** Virus load in the serum of mice after LCMV cl13 infection. *n* = 9. Data were pooled from two (A and B) or three (C) experiments. Statistical analysis was done with two-way ANOVA. Error bars show means ± SEM. *, P < 0.05; **, P < 0.01; ***, P < 0.001.

directly target Dnmt1 for destruction by proteasome (Nishiyama et al., 2013; Jia et al., 2016). All these observations suggest that the functions of Uhrf1 and Dnmt1 may be not fully redundant under certain conditions. Indeed, in our GC B cell–specific Uhrf1 KO mice, we did not detect increased double-strand DNA break by γH2A.X staining as the previous research did in Dnmt1-deficient mice (Shaknovich et al., 2011). The GC B cell survival in the absence of Uhrf1 was not affected either, further denoting the differential roles of Uhrf1 and Dnmt1 during GC B cell response.

Our data showed that the primary function of Uhrf1 is to promote cell proliferation by down-regulating cell proliferation inhibitors including Slfns and p21. More interestingly, we found that Uhrf1 was directly up-regulated by the c-Myc–AP4 axis, therefore correlating Uhrf1-dependent GC B cell proliferation with helper T cell–driven positive selection. Along with its impact on SHM, Uhrf1 critically ensures the GC affinity maturation, and Uhrf1 deficiency in GC B cells rendered the mice unable to control chronic LCMV infection. Notably, in terms of p21 regulation, in addition to its regulation by Uhrf1 showed in this study, p21 expression has also been reported to be directly inhibited by c-Myc and AP4 (Seoane et al., 2002; Wu et al., 2003; Jung et al., 2008; Jackstadt et al., 2013), emphasizing that appropriate p21 expression is so critical in GC response that it has to be stringently regulated at multiple layers.

Slfn family was first identified as a regulator of T cell development. The expression of Slfn1 is lower in immature proliferating thymocytes and up-regulated in quiescent single positive cells. Overexpression of Slfn1 leads to cell cycle arrest and disruption of T thymocyte maturation. Further studies showed that in addition to slfn1, slfn2 and slfn8 also play important roles in cell cycle inhibition and maintenance of cell quiescence. The function of Slfns had been well studied in T cells, natural killer cells, fibroblasts, and monocytes (Schwarz et al., 1998; Berger et al., 2010); however, the role of Slfns in B cells remains unknown. Our study suggests that Slfn proteins are critically involved in GC B cell response regulation. Uhrf1 mediates the DNA methylation of Slfn1 and Slfn2 in GC B cells. More interestingly, the mRNA expression and DNA methylation of Slfn2 during B cell differentiation is dynamic, with higher expression and lower DNA methylation in FoBs and vice versa in GC B cells. Up-regulated Uhrf1 in GC B cells actively represses Slfn2 via DNA methylation to promote cell proliferation.

Materials and methods

Mice

Uhrf1 floxed mice were provided by R. Huo (Nanjing Medical University, Nanjing, China). In brief, Uhrf1 floxed embryonic stem cells (colony name: EPD0052_1_G08) were obtained from the European Conditional Mouse Mutagenesis Program and microinjected into blastocysts of C57BL/6J mice. Mice were then crossed to FLPe transgenic mice to remove the neocassette and maintained on a C57BL/6J background. AID-Cre transgenic mice were provided by M. Busslinger (Research Institute of Molecular Pathology, Vienna, Austria) and B. Hou (Chinese Academy of Sciences, Beijing, China). All the control mice were littermate controls. Mice were housed in a specific pathogen-free environment in the Animal Core Facility of Nanjing Medical University or the Department of Laboratory Animal Science at Shanghai Medical College, Fudan University. Animal protocols were reviewed and approved by the Institutional Animal Care and Use Committee of Nanjing Medical University and the Institutional

Downloaded from http://rupress.org/jem/article-pdf/215/5/1437/1758913/jem_20171815.pdf by guest on 07 February 2026

Animal Care and Use Committee of Shanghai Medical College at Fudan University.

Cell culture and transduction

CH12F3 cells were provided by T. Honjo (Kyoto University, Kyoto, Japan) and Y. Zhang (National Institute of Biological Sciences, Beijing, China). The cells were cultured at 37°C with 5% CO_2 in RPMI-1640 medium with 10% (vol/vol) FBS (Gibco), 2 mM L-glutamine (Invitrogen), 1% penicillin/streptomycin (HyClone), 20 mM Hepes, 50 mM β-mercaptoethanol, and 5% (vol/vol) NCTC-109. For transient transduction, 2 µg of indicated plasmids were transfected into 1.5×10^6 CH12F3 cells following the Neon-Transfection System protocol. CD40L-expressing feeders were generated and used for B cell in vitro stimulation as described previously (Chou et al., 2016).

Flow cytometry

Lymphocytes were isolated from mouse spleen, mesenteric LNs, and Peyer's patches as described previously (Chen et al., 2017). For GC B cell staining, the following antibodies were from BioLegend: anti–B220-APC-Cy7 (RA3-6B2), anti–CD95-PE-Cy7 (Jo2), anti–IgD-APC or biotin (11-26c), anti–CD45.2-Aexa700 (104), and anti–CD45.1–Pacific blue (A20). Other antibodies were from BD: anti-AID (mAID-2), anti–GL7-APC or FITC or PE (GL7), antiactivated caspase 3–biotin (C92-605), anti–mouse IgG1-APC or FITC (A85-1), and anti–BrdU-APC or Alexa Fluor 488 (Bu20a). For Edu/BrdU double staining, anti-BrdU Alexa Fluor 488 (MoBU-1 clone; Invitrogen) was used. For Edu staining, the Edu staining kit from RiboBio was used. For the BrdU incorporation experiment, mice were intravenously injected with 2 mg BrdU (Sigma-Aldrich), and cells were stained with a BD BrdU flow kit (Bannard et al., 2016). For the GC B cell viability assay, cells were incubated in RPMI 1640 with 2% FBS at 37°C for 40 min before active caspase 3 staining.

Mouse immunization and LCMV infection

To induce the GC B cell response, mice were immunized with SRBCs or NP-KLH as described previously (Chen et al., 2017). For LCMV infection, mice were intravenously infected with 1×10^6 PFU of LCMV-clone13 or 2×10^5 PFU of LCMV-Armstrong. LCMV-Armstrong virus was provided by L. Ye (Third Military Medical University, Chongqing, China). For the quantification of serum viral load, RNA was extracted from serum of LCMV-infected mice using the ZR Viral RNA kit (Zymo Research) and subjected to RT-qPCR using NP2 primers (McCausland and Crotty, 2008).

RT-qPCR analysis

Total RNA was extracted using the RNeasy RNA isolation kit (QIAGEN) and reverse transcribed using the SuperScript First-strand synthesis system (Invitrogen). RT-qPCR was performed using SYBR green master mix (Vazyme). Gene specific primers are listed in the supplementary information.

Retroviral production and transduction

Mouse expression cDNAs were cloned into the MSCV-Thy1.1 retroviral vector, and shRNAs were cloned into the pSIREN-zsGreen vector. Virus was packaged in the PlatE cell line, and the viral supernatants were collected at 2 d after transfection. BM donor mice were treated with 5-FU for 5 d, and BM was collected for spin infection twice in the presence of 8 µg/ml polybrene (Sigma-Aldrich). Transduced BM cells were then intravenously transferred into lethally irradiated recipient mice to generate chimera mice. For B cell transduction, splenic B cells were stimulated with anti-CD180 for 24 h and then spin infected. shRNA sequences are included in Table S1.

ELISA

To quantify NP-specific antibodies, serum was collected at days 7, 14, and 21 after NP-KLH immunization. NP-specific high-affinity and low-affinity antibodies were captured on plates coated with 2.5 µg/ml NP4-BSA or NP41-BSA, respectively, as described previously (Chen et al., 2017).

Luciferase reporter assay

A region corresponding with the ~2-kb 5′-proximal segment of Uhrf1 (positions −800 to +1,200 of transcriptional start site) was amplified by PCR and subcloned into pGL3-basic (Promega). Selected point mutations aimed at the consensus AP4-binding sites were introduced. These constructs and a control reporter plasmid (pRL-SV40; Promega) were transfected together into HEK293T cells by lipofectamine (Thermo Fisher Scientific), together with plasmids encoding Flag-tagged mouse WT AP4. Luciferase expression was assessed 48 h later (Dual-Luciferase reporter kit; Promega).

ChIP assay

CH12F3 cells or GC B cells (1×10^7) were cross-linked with 1% formaldehyde, quenched with 0.125 M glycine, and washed in cold PBS. Cells were then lysed in lysis buffer (5 mM Tris-HCl, pH 8.1, 5 mM NaCl, 0.5% NP-40, and 1× PMSF) on ice, and sonicated to get a mean chromatin fragment length of 500 bp. 6 µg AP4 antibody or IgG was used for immunoprecipitation. After washing and elution, the DNA was purified with the EZ-ChIP DNA purification kit. qPCR was performed with SYBR green (Vazyme).

Western blotting

Western blot analysis was performed as previously described (Muppidi et al., 2014). In brief, cell lysates were separated by SDS-PAGE. Proteins were detected with antibodies against Uhrf1 (M-132; Santa Cruz Biotechnology), c-Myc (Y69; Abcam), AP4 (A-8; Santa Cruz Biotechnology), and β-actin (Cell Signaling Technology).

Immunohistochemistry

Spleens were cut into 8-µm cryosections and fixed with ice-cold acetone. Slides were blocked and incubated with primary antibodies and horseradish peroxidase or alkaline phosphatase–conjugated secondary antibodies. 3,3'-diaminobenzidine and Fast blue was used for development. For Uhrf1 staining, slides were permeabilized with 0.1% Triton X-100 before staining. Images were captured with an AxioObserver Z1 inverted microscope (ZEISS).

Dot blot analysis

Total 5mC was detected with dot blot analysis. Genomic DNA was extracted from sorted GC B cells and subjected to denaturation.

Downloaded from http://rupress.org/jem/article-pdf/215/5/1437/1758913/jem_20171815.pdf by guest on 07 February 2026

The single-strand DNA was bound and crossed-linked to a nitrocellulose membrane and detected with anti-5mC antibody (Cell Signaling Technology).

Bisulfite sequencing analysis

Genomic DNA from splenic B220$^+$Fas$^+$GL7$^+$ cells was extracted with an QIAamp DNA Micro kit and converted with the EpiTect Bisulfite kit (QIAGEN). Each DNA sample combined the mixture of DNA from at least three mice. Selected genomic regions were PCR-amplified by Taq HS enzyme (Vazyme). The PCR products were gel-purified using the Gel Extraction kit (Omega) and then cloned into pMD 20-T vector (Takara Bio Inc.) for sequencing.

The sequences of the Cdkn1a promoter primer sets were as follows: 5′-ATATGTTGGTTTTTGAAGAGGG-3′ and 5′-ATCCCAAAAAATCCCACTATATC-3′; Slfn1 promoter primer, 5′-TATTATTTTTATTGTTGTGGGTGTTT-3′ and 5′-ATCTAAATCCTCCTCAACCAATAATAA-3′; Slfn2 promoter primer, 5′-TAGTTAGGAGGATTTTGTAATAGGG-3′ and 5′-ACAAACTACAATCCAACTAACCCA-3′; and Slfn8 promoter primer, 5′-TTAGTATTTAGAAGGTTTTTTATTGGTTT-3′ and 5′-ATCTCTCACCCACTAAAATCATCC-3′.

Mutation analysis

The mutation analysis was performed as described previously (Chen et al., 2017). In brief, an intronic sequence 3′ to the JH4 exon of IgH and the VH186.2 sequences were PCR-amplified from genomic DNA extracted from 10,000 GC B cells. PCR products were cloned into pMD 20-T vector (Takara Bio Inc.) and sequenced. Obtained JH4 intronic sequences were aligned to the mm9 assembly of the mouse genomic sequence. VH186.2 sequences were validated with ImMunoGeneTics V-QUEST (http://www.imgt.org/).

Analysis of gene expression difference with RNA-seq

Control and *Uhrf1*$^{fl/fl}$AID-Cre$^+$ mice were infected with 10^6 PFU of LCMV-Armstrong, and splenic GC B cells (B220$^+$IgD^{low}CD95$^+$GL7$^+$) were FACS sorted 11 d later. RNA was obtained from 10^6 sorted GC B cells, and each RNA sample combined the mixture of RNA from three mice. RNA was subjected to Illumina HiSeq and PE150 sequencing performed by Vazyme. Sequence reads were mapped to the mm10 reference genome using Bowtie2 software, and fragments per kilobase per million were calculated with Cufflinks. The differential expressed genes were set with the threshold of $P < 0.05$ and fold change > 1.5 for volcano diagram and a threshold of $P < 0.05$ and fold change > 1.2 for GO-term pathway analysis and Venn diagram.

Statistical analysis

Student's *t* tests were used for bioinformatics analysis, unless Fisher's exact tests or ANOVA were used as indicated in the figure legends. Unless otherwise indicated, the data in figures are displayed as the mean ± SEM. P-values are denoted in figures by *, $P < 0.05$; **, $P < 0.01$; and ***, $P < 0.001$.

Data availability

The RNA-seq data were deposited in GEO under accession number GSE102270.

Online supplementary information

A list of qPCR primers and shRNA sequences can be found in Table S1. Further analysis of RNA-seq data are shown in Fig. S1. shRNA knockdown efficiency data are shown in Fig. S2. shRNA rescue experiments with mature B cells data are shown in Fig. S3.

Acknowledgments

We thank Dr. Lilin Ye for LCMV-Armstrong and Drs. Tasuku Honjo and Yu Zhang for CH12F3 cells.

This work was supported by National Natural Science Foundation of China grants 31570881 (to X. Wang), 81771670 (to X. Wang), and 31471107 (to R. Huo); the Thousand Talents plan; and Natural Science Foundation of Jiangsu Province grant BK20150992. X. Wang is a specially appointed professor by Universities in Jiangsu Province.

The authors declare no competing financial interests.

Author contributions: C. Chen and X. Wang conceptualized the project and designed the experiments. C. Chen, S. Zhai, L. Zhang, J. Chen, and X. Long performed the experiments. J. Qin, J. Li, and R. Huo provided the key reagents and mice. C. Chen and X. Wang analyzed the data and wrote the manuscript.

Submitted: 3 October 2017
Revised: 7 December 2017
Accepted: 1 March 2018

References

Allen, C.D.C., T. Okada, and J.G. Cyster. 2007. Germinal-center organization and cellular dynamics. *Immunity.* 27:190–202. https://doi.org/10.1016/j.immuni.2007.07.009

Bannard, O., S.J. McGowan, J. Ersching, S. Ishido, G.D. Victora, J.-S. Shin, and J.G. Cyster. 2016. Ubiquitin-mediated fluctuations in MHC class II facilitate efficient germinal center B cell responses. *J. Exp. Med.* 213:993–1009. https://doi.org/10.1084/jem.20151682

Bashtrykov, P., G. Jankevicius, R.Z. Jurkowska, S. Ragozin, and A. Jeltsch. 2014. The UHRF1 protein stimulates the activity and specificity of the maintenance DNA methyltransferase DNMT1 by an allosteric mechanism. *J. Biol. Chem.* 289:4106–4115. https://doi.org/10.1074/jbc.M113.528893

Basso, K., and R. Dalla-Favera. 2010. BCL6: master regulator of the germinal center reaction and key oncogene in B cell lymphomagenesis. *Adv. Immunol.* 105:193–210. https://doi.org/10.1016/S0065-2776(10)05007-8

Berger, M., P. Krebs, K. Crozat, X. Li, B.A. Croker, O.M. Siggs, D. Popkin, X. Du, B.R. Lawson, A.N. Theofilopoulos, et al. 2010. An Slfn2 mutation causes lymphoid and myeloid immunodeficiency due to loss of immune cell quiescence. *Nat. Immunol.* 11:335–343. https://doi.org/10.1038/ni.1847

Bergthaler, A., L. Flatz, A. Verschoor, A.N. Hegazy, M. Holdener, K. Fink, B. Eschli, D. Merkler, R. Sommerstein, E. Horvath, et al. 2009. Impaired antibody response causes persistence of prototypic T cell-contained virus. *PLoS Biol.* 7:e1000080. https://doi.org/10.1371/journal.pbio.1000080

Bergthorsdottir, S., A. Gallagher, S. Jainandunsing, D. Cockayne, J. Sutton, T. Leanderson, and D. Gray. 2001. Signals that initiate somatic hypermutation of B cells in vitro. *J. Immunol.* 166:2228–2234. https://doi.org/10.4049/jimmunol.166.4.2228

Bostick, M., J.K. Kim, P.-O. Estève, A. Clark, S. Pradhan, and S.E. Jacobsen. 2007. UHRF1 plays a role in maintaining DNA methylation in mammalian cells. *Science.* 317:1760–1764. https://doi.org/10.1126/science.1147939

Calado, D.P., Y. Sasaki, S.A. Godinho, A. Pellerin, K. Köchert, B.P. Sleckman, I.M. de Alborán, M. Janz, S. Rodig, and K. Rajewsky. 2012. The cell-cycle regulator c-Myc is essential for the formation and maintenance of

Downloaded from http://rupress.org/jem/article-pdf/215/5/1437/1758913/jem_20171815.pdf by guest on 07 February 2026

germinal centers. *Nat. Immunol.* 13:1092–1100. https://doi.org/10.1038/ni.2418

Chan, T.D., and R. Brink. 2012. Affinity-based selection and the germinal center response. *Immunol. Rev.* 247:11–23. https://doi.org/10.1111/j.1600-065X.2012.01118.x

Chen, J., Z. Cai, L. Zhang, Y. Yin, X. Chen, C. Chen, Y. Zhang, S. Zhai, X. Long, X. Liu, and X. Wang. 2017. Lis1 Regulates Germinal Center B Cell Antigen Acquisition and Affinity Maturation. *J. Immunol.* 198:4304–4311. https://doi.org/10.4049/jimmunol.1700159

Chou, C., D.J. Verbaro, E. Tonc, M. Holmgren, M. Cella, M. Colonna, D. Bhattacharya, and T. Egawa. 2016. The Transcription Factor AP4 Mediates Resolution of Chronic Viral Infection through Amplification of Germinal Center B Cell Responses. *Immunity.* 45:570–582. https://doi.org/10.1016/j.immuni.2016.07.023

Cui, Y., X. Chen, J. Zhang, X. Sun, H. Liu, L. Bai, C. Xu, and X. Liu. 2016. Uhrf1 Controls iNKT Cell Survival and Differentiation through the Akt-mTOR Axis. *Cell Reports.* 15:256–263. https://doi.org/10.1016/j.celrep.2016.03.016

De Silva, N.S., and U. Klein. 2015. Dynamics of B cells in germinal centres. *Nat. Rev. Immunol.* 15:137–148. https://doi.org/10.1038/nri3804

Dominguez-Sola, D., G.D. Victora, C.Y. Ying, R.T. Phan, M. Saito, M.C. Nussenzweig, and R. Dalla-Favera. 2012. The proto-oncogene MYC is required for selection in the germinal center and cyclic reentry. *Nat. Immunol.* 13:1083–1091. https://doi.org/10.1038/ni.2428

Espada, J., H. Peinado, L. Lopez-Serra, F. Setién, P. Lopez-Serra, A. Portela, J. Renart, E. Carrasco, M. Calvo, A. Juarranz, et al. 2011. Regulation of SNAIL1 and E-cadherin function by DNMT1 in a DNA methylation-independent context. *Nucleic Acids Res.* 39:9194–9205. https://doi.org/10.1093/nar/gkr658

Geserick, P., F. Kaiser, U. Klemm, S.H.E. Kaufmann, and J. Zerrahn. 2004. Modulation of T cell development and activation by novel members of the Schlafen (slfn) gene family harbouring an RNA helicase-like motif. *Int. Immunol.* 16:1535–1548. https://doi.org/10.1093/intimm/dxh155

Gitlin, A.D., Z. Shulman, and M.C. Nussenzweig. 2014. Clonal selection in the germinal centre by regulated proliferation and hypermutation. *Nature.* 509:637–640. https://doi.org/10.1038/nature13300

Gitlin, A.D., C.T. Mayer, T.Y. Oliveira, Z. Shulman, M.J.K. Jones, A. Koren, and M.C. Nussenzweig. 2015. HUMORAL IMMUNITY. T cell help controls the speed of the cell cycle in germinal center B cells. *Science.* 349:643–646. https://doi.org/10.1126/science.aac4919

Harker, J.A., G.M. Lewis, L. Mack, and E.I. Zuniga. 2011. Late interleukin-6 escalates T follicular helper cell responses and controls a chronic viral infection. *Science.* 334:825–829. https://doi.org/10.1126/science.1208421

Jackstadt, R., S. Röh, J. Neumann, P. Jung, R. Hoffmann, D. Horst, C. Berens, G.W. Bornkamm, T. Kirchner, A. Menssen, and H. Hermeking. 2013. AP4 is a mediator of epithelial-mesenchymal transition and metastasis in colorectal cancer. *J. Exp. Med.* 210:1331–1350. https://doi.org/10.1084/jem.20120812

Jia, Y., P. Li, L. Fang, H. Zhu, L. Xu, H. Cheng, J. Zhang, F. Li, Y. Feng, Y. Li, et al. 2016. Negative regulation of DNMT3A de novo DNA methylation by frequently overexpressed UHRF family proteins as a mechanism for widespread DNA hypomethylation in cancer. *Cell Discov.* 2:16007. https://doi.org/10.1038/celldisc.2016.7

Jung, P., A. Menssen, D. Mayr, and H. Hermeking. 2008. AP4 encodes a c-MYC-inducible repressor of p21. *Proc. Natl. Acad. Sci. USA.* 105:15046–15051. https://doi.org/10.1073/pnas.0801773105

Kent, B., E. Magnani, M.J. Walsh, and K.C. Sadler. 2016. UHRF1 regulation of Dnmt1 is required for pre-gastrula zebrafish development. *Dev. Biol.* 412:99–113. https://doi.org/10.1016/j.ydbio.2016.01.036

Kwon, K., C. Hutter, Q. Sun, I. Bilic, C. Cobaleda, S. Malin, and M. Busslinger. 2008. Instructive role of the transcription factor E2A in early B lymphopoiesis and germinal center B cell development. *Immunity.* 28:751–762. https://doi.org/10.1016/j.immuni.2008.04.014

Liang, C.C., B. Zhan, Y. Yoshikawa, W. Haas, S.P. Gygi, and M.A. Cohn. 2015. UHRF1 is a sensor for DNA interstrand crosslinks and recruits FAN CD2 to initiate the Fanconi anemia pathway. *Cell Reports.* 10:1947–1956. https://doi.org/10.1016/j.celrep.2015.02.053

Liu, F., P. Zhou, Q. Wang, M. Zhang, and D. Li. 2017. The Schlafen family: complex roles in different cell types and virus replication. *Cell Biol. Int.* 42:2–8.

Liu, X., Q. Gao, P. Li, Q. Zhao, J. Zhang, J. Li, H. Koseki, and J. Wong. 2013. UHRF1 targets DNMT1 for DNA methylation through cooperative binding of hemi-methylated DNA and methylated H3K9. *Nat. Commun.* 4:1563. https://doi.org/10.1038/ncomms2562

McCausland, M.M., and S. Crotty. 2008. Quantitative PCR technique for detecting lymphocytic choriomeningitis virus in vivo. *J. Virol. Methods.* 147:167–176. https://doi.org/10.1016/j.jviromet.2007.08.025

Mesin, L., J. Ersching, and G.D. Victora. 2016. Germinal Center B Cell Dynamics. *Immunity.* 45:471–482. https://doi.org/10.1016/j.immuni.2016.09.001

Muppidi, J.R., R. Schmitz, J.A. Green, W. Xiao, A.B. Larsen, S.E. Braun, J. An, Y. Xu, A. Rosenwald, G. Ott, et al. 2014. Loss of signalling via Gα13 in germinal centre B-cell-derived lymphoma. *Nature.* 516:254–258. https://doi.org/10.1038/nature13765

Nishiyama, A., L. Yamaguchi, J. Sharif, Y. Johmura, T. Kawamura, K. Nakanishi, S. Shimamura, K. Arita, T. Kodama, F. Ishikawa, et al. 2013. Uhrf1-dependent H3K23 ubiquitylation couples maintenance DNA methylation and replication. *Nature.* 502:249–253. https://doi.org/10.1038/nature12488

Obata, Y., Y. Furusawa, T.A. Endo, J. Sharif, D. Takahashi, K. Atarashi, M. Nakayama, S. Onawa, Y. Fujimura, M. Takahashi, et al. 2014. The epigenetic regulator Uhrf1 facilitates the proliferation and maturation of colonic regulatory T cells. *Nat. Immunol.* 15:571–579. https://doi.org/10.1038/ni.2886

Pérez-García, A., E. Marina-Zárate, Á.F. Álvarez-Prado, J.M. Ligos, N. Galjart, and A.R. Ramiro. 2017. CTCF orchestrates the germinal centre transcriptional program and prevents premature plasma cell differentiation. *Nat. Commun.* 8:16067. https://doi.org/10.1038/ncomms16067

Robertson, K.D., S. Ait-Si-Ali, T. Yokochi, P.A. Wade, P.L. Jones, and A.P. Wolffe. 2000. DNMT1 forms a complex with Rb, E2F1 and HDAC1 and represses transcription from E2F-responsive promoters. *Nat. Genet.* 25:338–342. https://doi.org/10.1038/77124

Schwarz, D.A., C.D. Katayama, and S.M. Hedrick. 1998. Schlafen, a new family of growth regulatory genes that affect thymocyte development. *Immunity.* 9:657–668. https://doi.org/10.1016/S1074-7613(00)80663-9

Seoane, J., H.-V. Le, and J. Massagué. 2002. Myc suppression of the p21(Cip1) Cdk inhibitor influences the outcome of the p53 response to DNA damage. *Nature.* 419:729–734. https://doi.org/10.1038/nature01119

Shaknovich, R., L. Cerchietti, L. Tsikitas, M. Kormaksson, S. De, M.E. Figueroa, G. Ballon, S.N. Yang, N. Weinhold, M. Reimers, et al. 2011. DNA methyltransferase 1 and DNA methylation patterning contribute to germinal center B-cell differentiation. *Blood.* 118:3559–3569. https://doi.org/10.1182/blood-2011-06-357996

Sharif, J., M. Muto, S. Takebayashi, I. Suetake, A. Iwamatsu, T.A. Endo, J. Shinga, Y. Mizutani-Koseki, T. Toyoda, K. Okamura, et al. 2007. The SRA protein Np95 mediates epigenetic inheritance by recruiting Dnmt1 to methylated DNA. *Nature.* 450:908–912. https://doi.org/10.1038/nature06397

Tian, Y., M. Paramasivam, G. Ghosal, D. Chen, X. Shen, Y. Huang, S. Akhter, R. Legerski, J. Chen, M.M. Seidman, et al. 2015. UHRF1 contributes to DNA damage repair as a lesion recognition factor and nuclease scaffold. *Cell Reports.* 10:1957–1966. https://doi.org/10.1016/j.celrep.2015.03.038

Wu, S., C. Cetinkaya, M.J. Munoz-Alonso, N. von der Lehr, F. Bahram, V. Beuger, M. Eilers, J. Leon, and L.-G. Larsson. 2003. Myc represses differentiation-induced p21CIP1 expression via Miz-1-dependent interaction with the p21 core promoter. *Oncogene.* 22:351–360. https://doi.org/10.1038/sj.onc.1206145

Xiang, H., L. Yuan, X. Gao, P.B. Alexander, O. Lopez, C. Lau, Y. Ding, M. Chong, T. Sun, R. Chen, et al. 2017. UHRF1 is required for basal stem cell proliferation in response to airway injury. *Cell Discov.* 3:17019. https://doi.org/10.1038/celldisc.2017.19

Zhang, H., H. Liu, Y. Chen, X. Yang, P. Wang, T. Liu, M. Deng, B. Qin, C. Correia, S. Lee, et al. 2016a. A cell cycle-dependent BRCA1-UHRF1 cascade regulates DNA double-strand break repair pathway choice. *Nat. Commun.* 7:10201. https://doi.org/10.1038/ncomms10201

Zhang, Y., L. Garcia-Ibanez, and K.-M. Toellner. 2016b. Regulation of germinal center B-cell differentiation. *Immunol. Rev.* 270:8–19. https://doi.org/10.1111/imr.12396

Zhao, J., X. Chen, G. Song, J. Zhang, H. Liu, and X. Liu. 2017. Uhrf1 controls the self-renewal versus differentiation of hematopoietic stem cells by epigenetically regulating the cell-division modes. *Proc. Natl. Acad. Sci. USA.* 114:E142–E151. https://doi.org/10.1073/pnas.1612967114

Downloaded from http://rupress.org/jem/article-pdf/215/5/1437/1758913/jem_20171815.pdf by guest on 07 February 2026